Chemiluminescent Probes for Activity-Based Sensing of Formaldehyde Released from Folate Degradation in Living Mice

Kevin J. Bruemmer[#a], **Ori Green**[#b], **Dr. Timothy A. Su**[#a], **Prof. Doron Shabat**[b], and **Prof. Christopher J. Chang**[a,c,d]

[a]Department of Chemistry, University of California, Berkeley, Berkeley, California 94720, United States cjchang@berkeley.edu

[b]School of Chemistry, Faculty of Exact Sciences, Tel Aviv University Tel Aviv 69978 (Israel) chdoron@post.tau.ac.il

[c]Department of Molecular and Cell Biology, University of California, Berkeley, Berkeley, California 94720, United States

[d]Howard Hughes Medical Institute, Chevy Chase, Maryland 20815, United States

[#] These authors contributed equally to this work.

Abstract

Formaldehyde (FA) is a common environmental toxin that is also produced naturally in the body through a wide range of metabolic and epigenetic processes, motivating the development of new technologies to monitor this reactive carbonyl species (RCS) in living systems. Here, we report a pair of first-generation chemiluminescent probes for selective formaldehyde detection. Caging phenoxy-dioxetane scaffolds bearing different electron-withdrawing groups with a general 2-aza-Cope reactive formaldehyde trigger provides Chemiluminescent Formaldehyde Probes 540 and 700 (**CFAP540** and **CFAP700**) for visible and near-IR detection of FA in living cells and mice, respectively. In particular, **CFAP700** is capable of visualizing FA release derived from endogenous folate metabolism, providing a starting point for the use of CFAPs and related chemical tools to probe FA physiology and pathology, as well as for the development of a broader palette of chemiluminescent activity-based sensing (ABS) probes that can be employed from in vitro biochemical to cell to animal models.

Graphical Abstract

COMMUNICATION

A first-generation set of chemiluminescent activity-based sensing probes for *in vivo* imaging of formaldehyde is reported. A formaldehyde-selective trigger is used to cage a phenol-dioxetane scaffold that emits a photon after aza-Cope-dependent uncaging. These reagents were utilized to image formaldehyde fluxes in living cells and mice, enabling the unique identification of endogenous formaldehyde production from metabolic folate cycles *in vivo*.

Supporting information for this article is given via a link at the end of the document.
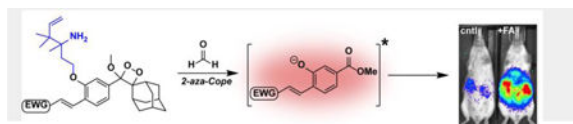
Keywords

Formaldehyde (FA) is a reactive carbonyl species (RCS) most commonly associated with being an external environmental pollutant, but it is also produced internally through a diverse array of biological processes.[1,2] This major one-carbon unit lies at the nexus of metabolism and epigenetics, participating in the synthesis of key biological molecules, including purines, amino acids, and neurotransmitters,[3–5] as well as in the methylation status of a variety of nucleic acid, protein, and small-molecule metabolites.[6–10]

The small and transient nature of FA has motivated growing interest in developing new activity-based sensing (ABS) methods[11–14] for selective FA detection,[15,16] including aza-Cope,[17–24] aminal, [25,26] and formimine [27–32] reaction-based triggers. Indeed, recent progress in developing fluorescent probes for FA detection in cells has elucidated more sophisticated biological roles for FA as both an exogenous toxin and an endogenous signaling molecule. Included is the discovery that FA is endogenously produced in the folate cycle through specific intermediates like tetrahydrofolate (THF) and 5,10-methyleneTHF, but not others like 5-methylTHF,[8] opening new doors to investigate the intriguing yet complex relationships between FA, methylation status and carcinogenesis. Despite these advances in fluorescent FA detection, FA imaging in living mammals is limited to an aza-Cope-based PET tracer,[33] which requires specialized equipment to implement. As such, we sought to develop a single, general platform for FA-selective ABS that would be applicable across a broader spectrum of biological models from *in vitro* biochemical to cell to *in vivo* animal systems. To this end, we turned our attention to chemiluminescent imaging, which offers an attractive approach in that it does not require external light irradiation, resulting in minimal background signal.[34–38] Here, we report first-generation chemiluminescent probes capable of visualizing changes in FA from *in vitro* to *in vivo* mouse models, offering a versatile approach to ABS of this central one-carbon molecule.

Our design relies upon a class of luminophores based on Schaap's dioxetane,[39,40] which has been exploited to create chemiluminescent probes for analytes spanning reactive oxygen/sulfur species[41–45] and enzyme activity.[43,46,47] Recent work from one of our labs has identified that introducing electron-withdrawing groups onto the *ortho* position of the phenol can result in a 1000-fold increase in chemiluminescence quantum efficiency and the ability to tune emission profiles,[43] particularly to the near-IR region to enable better tissue penetration for *in vivo* imaging.[48] Based on this scaffold, we created a set of chemiluminescent FA probes by caging this phenol with a 2-aza-Cope FA-reactive trigger (Scheme 1).[20] Chemiluminescent Formaldehyde Probes 540 and 700 (**CFAP540** and **CFAP700**) feature visible and near-IR emission profiles designed for *in vitro* cell and *in vivo* animal applications, respectively (see Supporting Information for synthetic details).

Reaction of FA at the homoallylamine, followed by immolation of the two-carbon linker through a β-elimination, yields the free phenol-dioxetane that subsequently decomposes through chemiexcitation to produce a photon.

With these CFAP reagents in hand, we first evaluated their chemiluminescent responses to FA (Figure 1) by adding a large excess of FA (10 mM) and measuring the light emission over several hours. The probes displayed a robust response to FA, with maximum light emission obtained within the first 60 minutes. **CFAP540** exhibits a maximum intensity increase of 500-fold compared to baseline (Figure 1a) with **CFAP700** showing a 33-fold intensity increase (Figure 1d). The lower observed turn-on response for **CFAP700** is likely due to minor off-pathway uncaging in buffered solution (Figure S5). To test responses to physiological concentrations of FA, the probes were exposed to 0, 10, 25, and 50 μM FA. Under these conditions, both **CFAP540** and **CFAP700** were capable of detecting 25–50 9μM levels of FA, with **CFAP540** capable of detecting 10 μM changes in FA due to its superior signal-to-noise response. Owing to their shared aza-Cope trigger, the CFAP reagents are highly selective for FA, with minimal emission observed upon reaction with other biologically-relevant aldehydes and molecules (Figure 1c, f).

With data showing that the probes are sensitive and selective for detecting FA in buffer, we next determined the ability of the CFAP platform to detect FA in living cells (Figure 2). HEK293 cells were first incubated with 10 μM **CFAP540** for 30 minutes in Dulbecco's Modified Eagle Medium (DMEM), then washed three times with phosphate-buffered saline (PBS) to remove excess probe. **CFAP700**, which lacks the esterase-sensitive methyl ester substituent found in **CFAP540**, is not cell-trappable under these repeated washing conditions and was not employed for cellular FA detection. Chemiluminescent signal was then measured for 90 minutes after exogenous addition of 0, 200, 500, or 1000 μM FA and showed a dose-dependent increase for **CFAP540**. Flow cytometry experiments confirm that the cells remain viable throughout the course of the experiment (Figure S8).

We then moved on to evaluate the CFAP platform for *in vivo* FA imaging in mouse models and utilized the red-shifted emission profile of **CFAP700** for deeper tissue penetration. We first sought to establish that **CFAP700** can detect exogenous FA addition in living animals in a dose-dependent manner. Anesthetized FVB-luc[+] mice received intraperitoneal (i.p.) injections of 0, 1.25, 2.5, 5, or 10 mg/kg FA in water; all doses are well below the LD_{50} range for FA reported for rodents.[49] The mice received subsequent i.p. injections of 100 μM **CFAP700**. Five minutes after injection, the mice were imaged with an IVIS luminescence instrument every 2.5 minutes over a 25-minute period. Figure 3a provides representative images of five mice injected with increasing amounts of FA. We observed a 1.8-fold increase at the lowest administered dose of 1.25 mpk, and a 28-fold increase at the highest administered dose (10 mpk), highlighting the significant dynamic range of the **CFAP700** probe for *in vivo* FA detection in these mouse models.

To support these results, we injected (i.p.) mice with either 2.5 mpk FA or water vehicle, then injected either 25 mpk sodium bisulfite as a FA scavenger or water vehicle, then injected 100 μM **CFAP700**. Mice that were injected with FA and sodium bisulfite showed no statistically significant difference in signal compared to the vehicle-treated control

(Figure 3c, d). We also found that bisulfite addition alone does not yield a discernable response from the vehicle control. These experiments further support the ability of **CFAP700** to detect changes in FA levels in living mice.

Finally, we demonstrated that the **CFAP700** probe is capable of detecting endogenous FA fluxes that are produced by the folate cycle, particularly through tetrahydrofolate metabolism (Figure 4). In these experiments, mice were injected with either vehicle (DMSO) or tetrahydrofolate (30 mpk), vehicle (water) or sodium bisulfite (25 mpk), and then 100 μM **CFAP700**. We observed an immediate difference at the first imaging point between the tetrahydrofolate- and vehicle-treated mice, which is consistent with the rapid rate of tetrahydrofolate metabolism detailed recently in cell models.[8]

In separate control experiments, we did not find any statistically significant differences between vehicle-treated mice and tetrahydrofolate-treated mice that were also exposed to the FA scavenger sodium bisulfite (25 mpk), which further establishes that the increased emission signal we observe upon tetrahydrofolate injection arises from the generation of FA from endogenous folate metabolism. Interestingly, we show that treatment with an equimolar quantity of aqueous calcium folinate (37 mpk) followed by **CFAP700** injection does not give any discernable difference in chemiluminescent signal over vehicle-treated mice (Figure S7). These data reveal that folinate and tetrahydrofolate, two important components of the folate cycle, show starkly different metabolic activities related to FA where folinate does not produce FA[50] and tetrahydrofolate is an effective FA producer *in vivo*.

To close, we have reported a first-generation pair of chemiluminescent probes for FA utilizing a general 2-aza-Cope FA-reactive trigger and a chemiluminegenic phenoxy-dioxetane scaffold. Functionalization at the *ortho*-position of the phenol yielded two distinct reagents that span the ability to monitor FA from *in vitro* biochemical to cell to *in vivo* animal models. Both **CFAP540** and **CFAP700** show high selectivity and sensitivity to FA, where the cell-trappability of **CFAP540** makes it suitable for cellular FA detection whereas the red-shifted emission profile of **CFAP700** can be exploited for live-animal FA visualization. Moreover, **CFAP700** provides the first *in vivo* evidence that folinate and tetrahydrofolate have distinct abilities to generate FA through folate cycle metabolism, presaging the utility of the CFAP platform and related chemical tools to help disentangle the complex pathways of FA production, metabolism, and signaling, particularly in the context of one-carbon biological chemistry. Finally, this work provides a general path forward to develop bright and tunable chemiluminescent ABS probes for a broader range of biological analytes that can be used in various types of specimens.

Supplementary Material

Refer to Web version on PubMed Central for supplementary material.

Acknowledgements

References

[1]. He RQ, Lu J, Miao JY, Sci. China Life Sci. 2010, 53, 1399–1404. [PubMed: 21181340]

[2]. Liteplo RG, Beauchamp R, Meek ME, Chénier R, Formaldehyde: Concise International Chemical Assessment Document 40, 2002.

[3]. Tibbetts AS, Appling DR, Annu. Rev. Nutr. 2010, 30, 57–81. [PubMed: 20645850]

[4]. Locasale JW, Nat. Rev. Cancer 2013, 13, 572–583. [PubMed: 23822983]

[5]. Tedeschi PM, Markert EK, Gounder M, Lin H, Dvorzhinski D, Dolfi SC, Chan LLY, Qiu J, DiPaola RS, Hirshfield KM, et al., Cell Death Dis. 2013, 4, e877. [PubMed: 24157871]

[6]. Ehrlich M, Oncogene 2002, 21, 5400–5413. [PubMed: 12154403]

[7]. Lu SC, Mato JM, Physiol. Rev. 2012, 92, 1515–1542. [PubMed: 23073625]

[8]. Burgos-Barragan G, Wit N, Meiser J, Dingler FA, Pietzke M, Mulderrig L, Pontel LB, Rosado IV, Brewer TF, Cordell RL, et al., Nature 2017, 548, 549–554. [PubMed: 28813411]

[9]. Hamm S, Just G, Lacoste N, Moitessier N, Szyf M, Mamer O, Bioorganic Med. Chem. Lett. 2008, 18, 1046–1049.

[10]. Walport LJ, Hopkinson RJ, Schofield CJ, Curr. Opin. Chem. Biol. 2012, 16, 525–534. [PubMed: 23063108]

[11]. Chan J, Dodani SC, Chang CJ, Nat. Chem. 2012, 4, 973–984. [PubMed: 23174976]

[12]. Lee MH, Kim JS, Sessler JL, Chem. Soc. Rev. 2015, 44, 4185–4191. [PubMed: 25286013]

[13]. Chen X, Tian X, Shin I, Yoon J, Chem. Soc. Rev. 2011, 40, 4783. [PubMed: 21629957]

[14]. Yang Y, Zhao Q, Feng W, Li F, Chem. Rev. 2013, 113, 192–270. [PubMed: 22702347]

[15]. Bruemmer KJ, Brewer TF, Chang CJ, Curr. Opin. Chem. Biol. 2017, 39, 17–23. [PubMed: 28527906]

[16]. Xu Z, Chen J, Hu L-L, Tan Y, Liu S-H, Yin J, Chinese Chem. Lett. 2017, 28, 1935–1942.

[17]. Brewer TF, Chang CJ, J. Am. Chem. Soc. 2015, 137, 10886–10889. [PubMed: 26306005]

[18]. Roth A, Li H, Anorma C, Chan J, Brewer TF, Chang CJ, Roth A, Li H, Anorma C, Chan J, J. Am. Chem. Soc. 2015, 137, 10890–10893. [PubMed: 26305899]

[19]. Liu W, Truillet C, Flavell RR, Brewer TF, Evans MJ, Wilson DM, Chang CJ, Chem. Sci. 2016, 7, 5503–5507. [PubMed: 30034690]

[20]. Bruemmer KJ, Walvoord RR, Brewer TF, Burgos-Barragan G, Wit N, Pontel LB, Patel KJ, Chang CJ, J. Am. Chem. Soc. 2017, 139, 5338–5350. [PubMed: 28375637]

[21]. Brewer TF, Burgos-Barragan G, Wit N, Patel KJ, Chang CJ, Chem. Sci. 2017, 8, 4073–4081. [PubMed: 28580121]

[22]. Dou K, Chen G, Yu F, Liu Y, Chen L, Cao Z, Chen T, Li Y, You J, Chem. Sci. 2017, 8, 7851–7861. [PubMed: 29163922]

[23]. Zhou Y, Yan J, Zhang N, Li D, Xiao S, Zheng K, Sensors Actuators B Chem. 2018, 258, 156–162.

[24]. W. X and Xilei Xie BT, Tang Fuyan, Shangguan Xiaoyan, Che Shiyi, Niu Jinye, Xiao Yongsheng, Chem. Commun. 2017, 53, 6520–6523.

[25]. Liu C, Jiao X, He S, Zhao L, Zeng X, Dye. Pigment. 2017, 138, 23–29.

[26]. He L, Yang X, Ren M, Kong X, Liu Y, Lin W, Chem. Commun. 2016, 52, 9582–9585.

[27]. Xie Z, Ge J, Zhang H, Bai T, He S, Ling J, Sun H, Zhu Q, Sensors Actuators B Chem. 2017, 241, 1050–1056.

[28]. Tang Y, Kong X, Xu A, Dong B, Lin W, Angew. Chemie - Int. Ed. 2016, 55, 3356–3359.

[29]. Wu F, Zhang Y, Huang L, Xu D, Wang H, Anal. Methods 2017, 9, 5472–5477.

[30]. Lee YH, Tang Y, Verwilst P, Lin W, Kim JS, Chem. Commun. 2016, 52, 11247–11250.

[31]. Tang Y, Kong X, Liu Z-R, Xu A, Lin W, Anal. Chem. 2016, 88, 9359–9363. [PubMed: 27653930]

[32]. Song X, Han X, Yu F, Zhang J, Chen L, Lv C, Analyst 2018, 143, 429–439. [PubMed: 29260163]

[33]. Liu W, Truillet C, Flavell RR, Brewer TF, Evans MJ, Wilson DM, Chang CJ, Chem. Sci. 2016, 7, 5503–5507. [PubMed: 30034690]

[34]. Lippert AR, ACS Cent. Sci. 2017, 3, 269–271. [PubMed: 28470041]

[35]. Hananya N, Shabat D, Angew. Chemie - Int. Ed. 2017, 56, 16454–16463.

[36]. Dodeigne C, Thunus L, Lejeune R, Talanta 2000, 51, 415–439. [PubMed: 18967873]

[37]. Gnaim S, Green O, Shabat D, Chem. Commun. 2018, 54, 2073–2085.

[38]. Li X, Gao X, Shi W, Ma H, Chem. Rev. 2014, 114, 590–659. [PubMed: 24024656]

[39]. Schaap AP, Chen T, Handley RS, Tetrahedron Lett. 1987, 28, 1155–1158.

[40]. Thurnauer MC, Bowman MK, Cope BT, Norris JR, J. Am. Chem. Soc. 1978, 100, 1966–1968.

[41]. Hananya N, Green O, Blau R, Satchi-Fainaro R, Shabat D, Angew. Chemie Int. Ed. 2017, 56, 11793–11796.

[42]. Cao J, Lopez R, Thacker JM, Moon JY, Jiang C, Morris SNS, Bauer JH, Tao P, Mason RP, Lippert AR, Chem. Sci. 2015, 6, 1979–1985. [PubMed: 25709805]

[43]. Green O, Eilon T, Hananya N, Gutkin S, Bauer CR, Shabat D, ACS Cent. Sci. 2017, 3, 349–358. [PubMed: 28470053]

[44]. Cao J, An W, Reeves AG, Lippert AR, Chem. Sci. 2018, 9, 2552–2558. [PubMed: 29732134]

[45]. Sun S, Bao Z, Ma H, Zhang D, Zheng X, Biochemistry 2007, 46, 6668–6673. [PubMed: 17497889]

[46]. Roth-Konforti ME, Bauer CR, Shabat D, Angew. Chemie Int. Ed. 2017, 56, 15633–15638.

[47]. Cao J, Campbell J, Liu L, Mason RP, Lippert AR, Anal. Chem. 2016, 88, 4995–5002. [PubMed: 27054463]

[48]. Green O, Gnaim S, Blau R, Eldar-Boock A, Satchi-Fainaro R, Shabat D, J. Am. Chem. Soc. 2017, 139, 13243–13248. [PubMed: 28853880]

[49]. Duong A, Steinmaus C, McHale CM, Vaughan CP, Zhang L, Mutat. Res. - Rev. Mutat. Res. 2011, 728, 118–138.

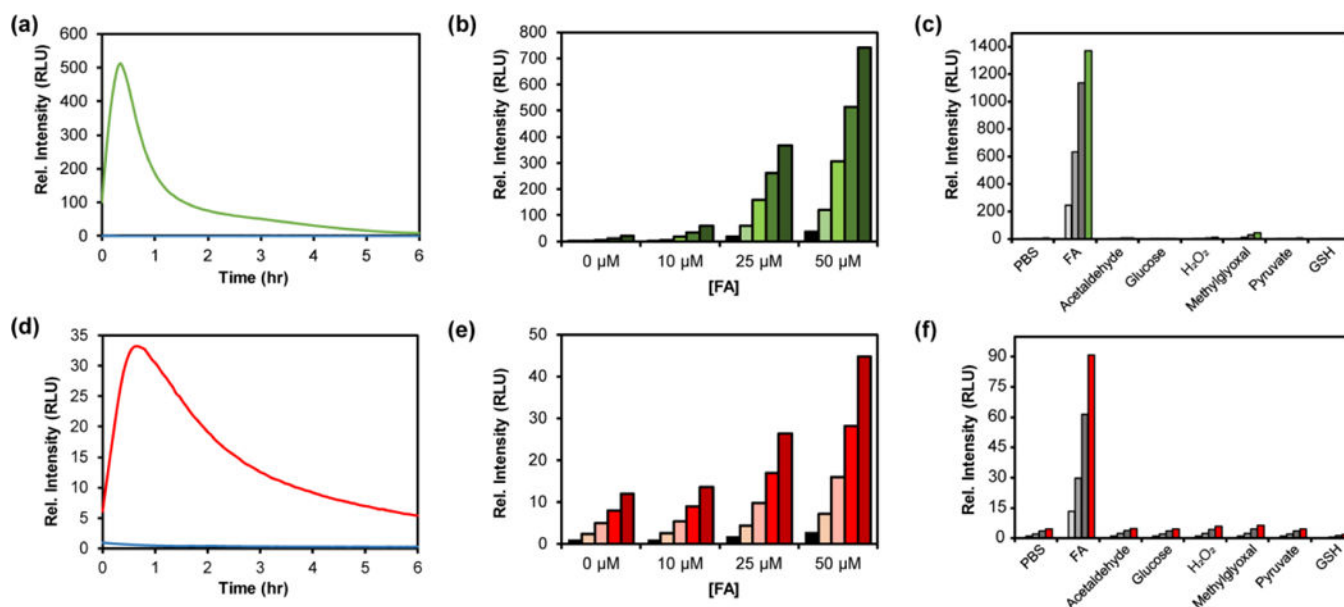[50]. Scaglione F, Panzavolta G, Xenobiotica 2014, 44, 480–488. [PubMed: 24494987]

Figure 1.
(a,d) Chemiluminescence kinetic profiles of 10 μM **(a) CFAP540** or **(d) CFAP700** to 0 μM
FA (blue trace) and 10 mM FA (green or red trace) in PBS (10 mM, pH 7.4, 10% FBS) at
37°C. **(b,d)** Chemiluminescence responses of 10 μM **(b) CFAP540** or **(e) CFAP700** to 0, 10,
25 and 50 μM FA. Data were acquired in DMEM growing media at 37 °C. Bars represent
time points taken at 0 (black), 30, 60, 120 and 240 min (green or red) after addition of FA.
(c,f) Chemiluminescence responses of 10 μM **(c) CFAP540** or **(f) CFAP700** to RCS or
relevant biological analyte. Bars represent emission intensity responses to 100 μM analyte
for 0 (lightest gray), 30 (light gray), 60 (gray), 90 (dark gray), and 120 (colored) min.
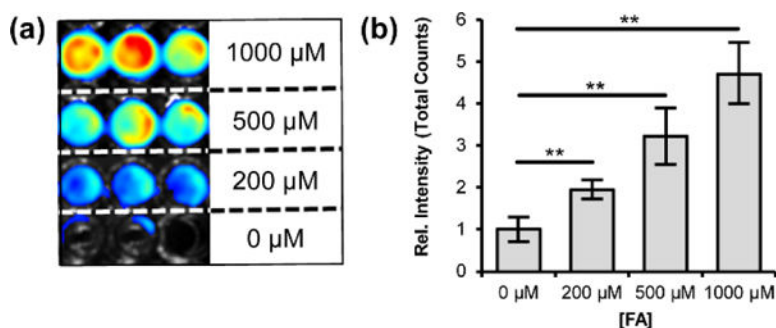
Figure 2.
Chemiluminescence detection of FA in live cells with **CFAP540**. HEK293 cells were treated with **CFAP540** (10 μM, 0.1% DMSO) and incubated for 30 minutes in growth medium. Growth medium was removed and cells were washed thrice with PBS (pH 7.4) Then, cells were treated with 0, 200, 500 and 1000 μM formaldehyde and the chemiluminescence signal was collected for 90 minutes. **(a)** Representative chemiluminescence cell images in triplicate. **(b)** Quantification of total light emitted from the cells after 90 minutes. Error bars are ±SEM (n = 6), and statistical analyses were performed with a two-tailed Student's t test where **P ≤ 0.01.
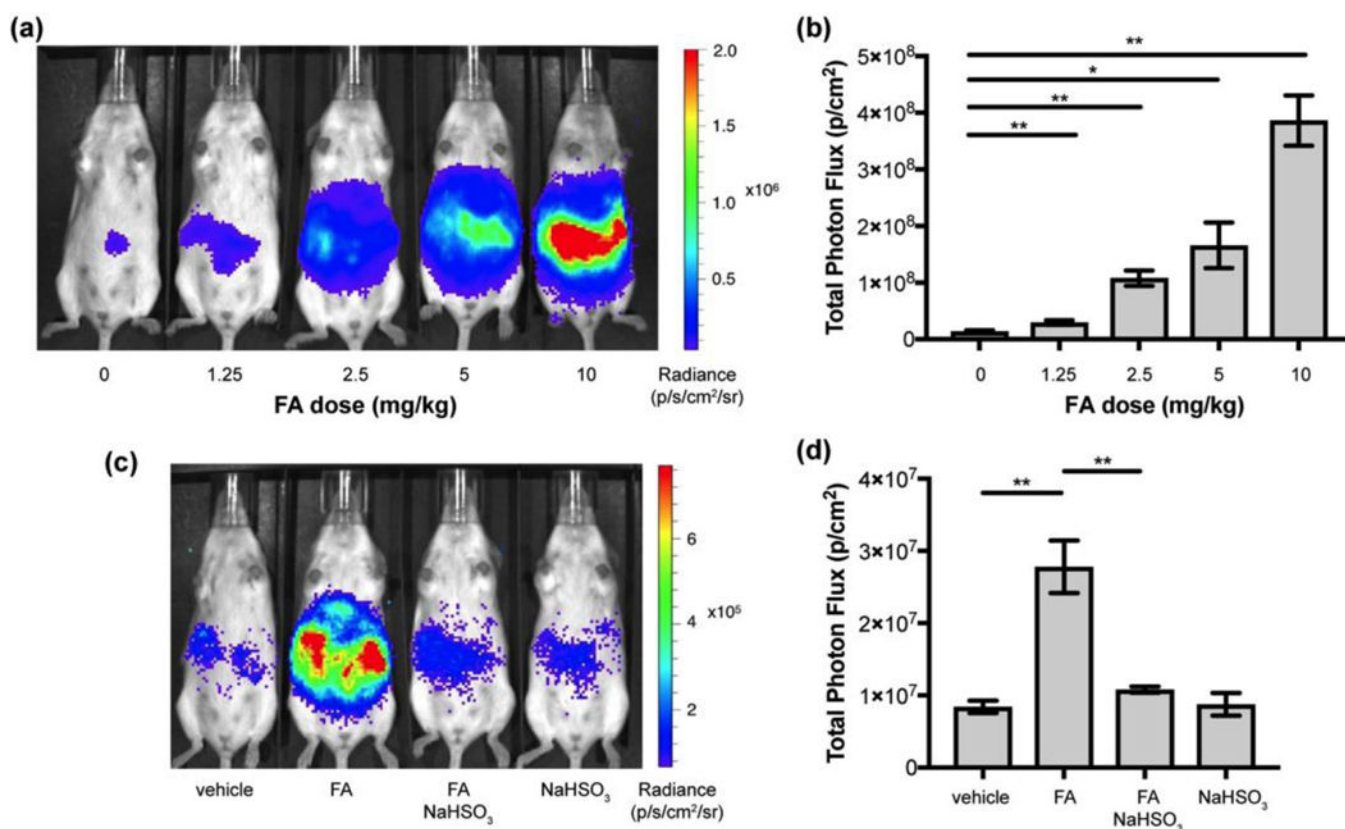
Figure 3.
Chemiluminescent imaging of **CFAP700** in response to exogenous FA and FA scavenger treatment. FVB-luc+ mice were injected (i.p.) with FA in water, then injected with 100 μM **CFAP700** (100 μL, 1% DMSO, 1% BSA in PBS). The mice were imaged every 2.5 minutes from 0–25 mins. **(a)** Representative images of FVB-luc+ mice injected with the FA probe and varying doses of FA. **(b)** Total photon flux, integrated from 0–25 min post injection with region of interest over the intraperitoneal cavity. Error bars are ±SEM (n = 3) **(c)** FVB-luc+ mice were injected (i.p.) with aqueous FA (2.5 mpk) or water, then aq. sodium bisulfite (25 mpk) or water, then 100 μM FAP-700 (100 μL). Representative images of FVB-luc+ mice injected with FA probe, FA, and/or sodium bisulfite. **(d)** Total photon flux, integrated from 0–25 min post injection. Error bars are ±SEM (n = 3–4). **(b,d)** Statistical analyses were performed with a two-tailed Student's t test where *P   0.05,**P   0.01.
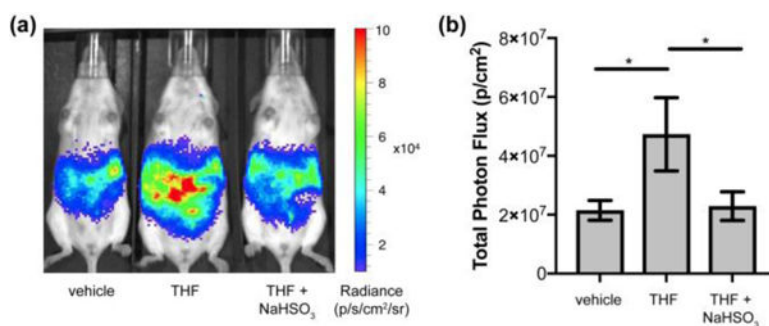
Figure 4.
CFAP700 can detect endogenous FA generated via tetrahydrofolate metabolism. FVB-luc+ mice were injected (i.p.) with tetrahydrofolate (30 mpk) or DMSO, then aq. sodium bisulfite (25 mpk) or water, then 100 μM **CFAP700** (100 μL, 1% DMSO, 1% BSA in PBS). The mice were imaged every 2.5 minutes from 0–25 min. **(a)** Representative images of FVB-luc + mice injected with **CFAP700**, THF, and/or bisulfite. **(b)** Total photon flux, integrated from 0–25 min post injection. Error bars are ±SEM (n = 4–5). Statistical analyses were performed with a two-tailed Student's t test where *P ≤ 0.05.
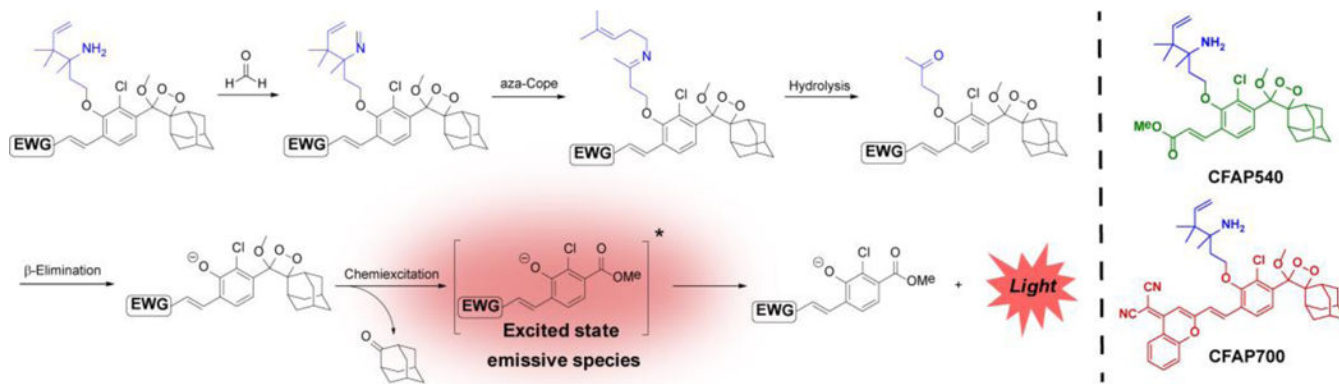
Scheme 1.
Reaction pathway of the 2-aza-Cope trigger followed by chemiexcitation of CFAP probes allows for the detection of formaldehyde. Chemical structures of **CFAP540** and **CFAP700**.